Simple Chaotic Oscillator: From Mathematical Model to Practical Experiment

Jiří PETRŽELA, Zdeněk KOLKA, Stanislav HANUS

Dept. of Radio Electronics, Brno University of Technology, Purkyňova 118, 612 00 Brno, Czech Republic

xpetrz07@stud.feec.vutbr.cz

Abstract. *This paper shows the circuitry implementation and practical verification of the autonomous nonlinear oscillator. Since it is described by a single third-order differential equation, its state variables can be considered as the position, velocity and acceleration and thus have direct connection to a real physical system. Moreover, for some specific configurations of internal system parameters, it can exhibit a period doubling bifurcation leading to chaos. Two different structures of the nonlinear element were verified by a comparison of numerically integrated trajectory with the oscilloscope screenshots.*

Keywords

Nonlinear oscillator, chaos, Lyapunov exponents, circuit realization, measurement.

1. Introduction

It is well known that many physical systems with some time evolution can be described by a set of generally nonlinear differential equations. It seems that an electronic circuit is an easy way how to construct a dynamical system which represents a given mathematical model. That is why we often use this approach for the purpose of studying dynamical motion, which can be simple (fixed points, limit cycles) as well as very complicated (chaos). We can also see some universality behind the construction of chaotic oscillators, because we are not interested in the concrete physical interpretation of the individual state variables.

For example, chaos was recently reported in the scientific fields such as chemistry, mechanics, economy, biology, etc. For lumped electronic circuit, the necessary condition is a finite number of the state variables and, of course, a complexity of the synthesized network grows in accordance with growing dimension of the dynamical system. The very first discovered chaotic oscillator was deeply described in [1], and is so far the only dynamical system where the presence of chaos was confirmed numerically, experimentally as well as mathematically. These equations, taking name after its discoverer as the Chua´s equations, belong to extensive group of dynamical systems covered by a following state space representation in compact matrix form

$$\dot{\mathbf{x}} = \mathbf{A}\,\mathbf{x} + \mathbf{b}\,h\left(\mathbf{w}^T\mathbf{x}\right) \tag{1a}$$

where $\mathbf{x}\in\Re^3$ is a vector of the state variables, $\mathbf{A}$ is a square matrix and $\mathbf{b}$, $\mathbf{w}$ are column vectors. The saturation-type nonlinearity of the form

$$h\left(\mathbf{w}^T\mathbf{x}\right) = 0.5\left(\left|\,\mathbf{w}^T\mathbf{x}+1\,\right| - \left|\,\mathbf{w}^T\mathbf{x}-1\,\right|\right), \tag{1b}$$

separates the state space by two parallel boundary planes $U_{\pm 1}$ into the three affine regions making a brief analysis possible and quite simple. Due to the symmetrical vector field with respect to the origin, the dynamical behavior in both outer regions $D_{\pm 1}$ of the state space is the same and determined by the roots of the characteristic polynomial

$$\begin{aligned}\det\left(s\,\mathbf{E}-\mathbf{A}\right) &= \left(s-\upsilon_1\right)\left(s-\upsilon_2\right)\left(s-\upsilon_3\right) = \\ &= s^3 - q_1 s^2 + q_2 s - q_3 = 0\,,\end{aligned} \tag{2a}$$

and similarly for single inner region D_0

$$\begin{aligned}\det\left[\,s\,\mathbf{E}-\left(\mathbf{A}+\mathbf{b}\,\mathbf{w}^{\mathbf{T}}\right)\,\right] &= \left(s-\mu_1\right)\left(s-\mu_2\right)\left(s-\mu_3\right) = \\ &= s^3 - p_1 s^2 + p_2 s - p_3 = 0\,,\end{aligned} \tag{2b}$$

where $\mathbf{E}$ is the unity matrix. In the parameter space of some interest we can assume one fixed point per state space region, namely

$$\left(\mathbf{A}+\mathbf{b}\,\mathbf{w}^{\mathbf{T}}\right)\bar{\mathbf{x}}_{inner} = \mathbf{0} \rightarrow \bar{\mathbf{x}}_{inner} = \begin{pmatrix}0 & 0 & 0\end{pmatrix}^T, \tag{3a}$$

and

$$\bar{\mathbf{x}}_{outer} = \pm\mathbf{A}^{-1}\mathbf{b}\,, \quad \det\left(\mathbf{A}\right) \neq 0\,. \tag{3b}$$

The main property of the chaotic solution is in extreme sensitivity to the changes of the initial conditions. It implies that we can not obtain closed-form analytic solution, so our analysis is restricted to the numerical integration. There is always some uncertainty in the initial state so that any predictions about future behavior are no longer available. Moreover, the chaotic attractor is dense having a fractional topological dimension. No-intersection theorem means that for chaos there must be at least three state variables.

2. Mathematical Model

Note that the dynamical system expressed as (1) is linear in each region of the state space, with the behavior given uniquely by eigenvalues, roots of the characteristic polynomial. To model any type of motion of such a class of dynamical systems, the parameter space must be at least six-dimensional. Now, we try to reduce this amount as much as possible, preserving a global qualitative behavior. To specify the parameter window where the chaos becomes possible, we should first recall the relations between eigenvalues and their equivalent numbers p_i´s and q_i´s. Substituting $s=\alpha_1/3+\Lambda$ into (2) leads to a reduced cubic polynomial of the form

$$\Lambda^3+\frac{3\alpha_2-\alpha_1^2}{9}\Lambda+\eta=0 \tag{4}$$

where

$$\eta=\frac{\alpha_1\alpha_2}{6}-\frac{\alpha_3}{2}-\frac{\alpha_1^{\,3}}{27}. \tag{5}$$

Let denote

$$\Delta=\frac{\alpha_3^2}{4}-\frac{\alpha_1^2\alpha_2^2}{108}+\frac{\alpha_1^3\alpha_3}{27}-\frac{\alpha_1\alpha_2\alpha_3}{6}+\frac{\alpha_2^3}{27}. \tag{6a}$$

and

$$\psi_{pos,neg}=\sqrt[3]{-\eta+\sqrt{\Delta}}\pm\sqrt[3]{-\eta-\sqrt{\Delta}}\,. \tag{6b}$$

For $\Delta>0$ we have one real

$$\lambda_3=\psi_{pos}+\alpha_1/3, \tag{7}$$

and a pair of complex conjugated numbers $\sigma\pm\omega i$ with the following real and imaginary part

$$\sigma=-\psi_{pos}/2+\alpha_1/3,\quad \omega=\sqrt{3}\,\psi_{neg}/2. \tag{8}$$

In these terms $\alpha_i=p_i$ or $\alpha_i=q_i$ depending on the region of the state space. The relations between eigenvalues and their equivalent numbers are given by the formulas

$$\begin{aligned}&2\sigma+\lambda_3=\alpha_1,\quad \lambda_3\left(\sigma^2+\omega^2\right)=\alpha_3,\\ &\sigma^2+\omega^2+2\sigma\lambda_3=\alpha_2.\end{aligned} \tag{9}$$

In the case of double-scroll attractor, state space geometry is $D_{\pm1}$: $\mathfrak{R}_u^{\,2}\oplus\mathfrak{R}_s^{\,1}$ and D_0: $\mathfrak{R}_u^{\,1}\oplus\mathfrak{R}_s^{\,2}$ while for producing the so-called double-hook attractor it should be $D_{\pm1}$: $\mathfrak{R}_u^{\,2}\oplus\mathfrak{R}_s^{\,1}$ together with D_0: $\mathfrak{R}_u^{\,1}\oplus\mathfrak{R}_s^{\,1}\oplus\mathfrak{R}_s^{\,1}$. In spite of the obvious restrictions of the eigenvalues resulting from the terms (9), the inner region can behave like an overdamped circuit. To date, no double-hook attractor produced by a nonlinear oscillator was reported. Searching for such a configuration of system parameters leading to some structure of chaotic attractor [6] is the topic of our future study.

The process of reduction of internal system parameters is based on the equivalence of some pair q_i and p_i with the same order. Since the parameter α_3 directly corresponds to λ_3 we have immedietely

$$\lambda_3^{\,outer}<0\rightarrow q_3<0,\quad \lambda_3^{\,inner}>0\rightarrow p_3>0, \tag{10}$$

leading to the condition $q_3\neq p_3$. If this is satisfied, there is just one equilibrium point per region as necessary for generation of chaotic attractors. Starting with the reference dynamical system of class C presented in [2] and taking into account $q_1=p_1$ and $q_2=p_2$ we can write the differential equations describing the new dynamical system as

$$\begin{aligned}&dx/dt=y,\quad dy/dt=z,\\ &dz/dt=q_1z-q_2y+g(x),\end{aligned} \tag{11}$$

where the piecewise-linear (PWL) function

$$g(x)=q_3x+(p_3-q_3)h(x). \tag{12}$$

The fixed points located inside regions $D_{\pm1}$ migrate along the x axis with the ratio

$$\overline{\mathbf{x}}_{outer}=\left(\pm\,p_3/q_3\mp1\quad 0\quad 0\right)^T. \tag{13}$$

Note that these fixed points can eventually enter D_0 region. It is evident that $q_3\neq0$. Similarly, $p_3\neq0$ otherwise there is an equilibrium line in the inner state space segment. Due to the dissipativity of the system, one must have $q_1<0$. Next, let write a basic conditions using a signum function, i.e. $\mathrm{sign}(\sigma_{\mathrm{inner}})\neq\mathrm{sign}(\sigma_{\mathrm{outer}})$ and $\sigma_{\mathrm{inner}}<0$. Then, terms (9) lead to

$$q_2<\sigma^2+\omega^2,\quad q_1>\lambda_3^{\,outer}. \tag{14}$$

Note that all conditions above are in accordance with a formation of hyperbolic equilibria, where $\sigma\neq0$. To preserve $\sigma_{\mathrm{outer}}>0$, i.e. the saddle-focus of index 2 equilibria in $D_{\pm1}$ we have $\psi_{pos}<min(-q_1/3,\ 2q_1/3)$. The process of double-scroll attractor evolution is briefly discussed by means of Fig. 4. It is evident that both boundary planes $U_{\pm1}$ can not be coplanar with any eigenplane denoted as eP or eigenvector marked as eV. Nevertheless, to acquire a better overview on the global dynamics, one can make a linear transformation of coordinates. For example, if the state matrix is in a real Jordan form, eV is orthogonal to eP. In spite of this, making a rigorous mathematical proof of chaos is a nontrivial task. Here, we simply suppose that the so-called Shilnikov´s theorems [7] are fulfilled, its detailed form will be given elsewhere. In further text, we adopt the following constant set of the parameters

$$q_1=-0.6,\quad q_2=0.846. \tag{15}$$

The same numbers also appear in [3]. Now, let see what eigenvalues hold for the partial cases of the Fig. 4. For the first picture it is $\sigma_{\mathrm{outer}}=-0.05$, $\lambda_3^{\mathrm{outer}}=-0.502$, $\sigma_{\mathrm{inner}}=-0.572$, $\lambda_3^{\mathrm{inner}}=0.545$ and for the last picture the corresponding eigenvalues are $\sigma_{\mathrm{outer}}=0.171$, $\lambda_3^{\mathrm{outer}}=-0.942$, $\sigma_{\mathrm{inner}}=-0.572$, $\lambda_3^{\mathrm{inner}}=0.545$.

Let define the volume element in the tangent space of the vector field. We can classify the type of the attractor by using the concept of one-dimensional Lyapunov exponent (LE), which measures the average rate of the convergence or divergence of two neighborhood trajectories. There are just three LE and, in accordance with the natural definition of chaos, one LE must be positive and one equals to zero. Because of the dissipation, the last one must be negative with the largest absolute value, as the element is shrinking with the time progression. Fig. 1 and Fig. 2 illustrate how the largest one-dimensional LE varies with the two natural bifurcation parameters p_3 and q_3 (with respect to circuit). Each of these graphs consist of 10201 point, computed for final time t_{max}=400. A standard Gram-Smith orthogonalization were performed during the estimation after each Δt=1 step. The significance of colors is shown in Fig. 2. From this point of view, light blue marks a trivial fixed point and inside the white areas entire solution suddenly becomes unbounded. Selected state trajectories of some interest were also numerically simulated by using MathCAD and build-in 4th order Runge-Kutta iteration method with time interval $t\in(0, 600)$, iteration step Δ=0.06 and initial conditions $\mathbf{x}_o=(0.5\ \ 0\ \ 0)^T$. The results are shown in Fig. 3, with color scale growing along the vertical axis.

3. Circuitry Implementation

The algebraical simplicity of the differential equations does not guarantee also its easy physical implementation. In spite of this, the new dynamical system (11) has one big advantage if compared to a classical first ODE equivalent of Chua´s equation [4]. It is much more easy to practically realize (11) with four independent parameters than a system with six parameters. The straightforward circuit synthesis is usually based on basic building blocks such as inverting integrator, differential amplifiers and PWL transfer function. Such realization leads to a large number of circuit elements. Here, we are going to use a completely different approach. It is evident that we can recast (11) into the single differential equation of the third-order. Thus, we can realize this dynamical system by parallel connection of the third-order admittance function together with a nonlinear resistor having PWL or polynomial AV curve. For admittance function shown in Fig. 5 we can derive the expression

$$Y(s)=C_1C_2C_3R_1R_2s^3+C_1C_2(R_1+R_2)s^2+(C_1+C_2)s.$$

To obtain a common-valued circuit elements, a current and time rescaling have been performed leading to following listing of linear capacitors and resistors

$$C_1=C_2=5\text{ nF},\ C_3=16\text{ nF},\ R_1=10\text{ k}\Omega,\ R_2=20\text{ k}\Omega, \quad (17)$$

and operational amplifier AD713. For experimental verification, we suppose that (17) does not change. Two different configurations of the active nonlinear resistor have been used, i.e. PWL resistor shown in Fig. 6 and polynomial resistor with the structure given by Fig. 7. In the first case, 1N4007 diodes and current-feedback amplifier AD844 has been used to form a basic negative slope of the final AV curve. The voltages of two independent external dc sources should be chosen carefully low to preserve CFOA working in the linear regime.

Let consider some level of idealization resulting into the equations

$$U^+=U^-,\quad I^-=I^C,\quad I^+=0,\quad U^C=U^O. \quad (18)$$

The input admittance of the PWL resistor in the region D_0 then becomes

$$Y_{input}=-1/R_{neg}, \quad (19a)$$

while in both outer segments of the vector field it is

$$Y_{input}=1/(R_{slope}+R_d)-1/R_{neg}, \quad (19b)$$

where R_d is a differential resistance of a diode in the forward direction. We can derive the fundamental condition for the existence of three fixed points in the form $R_{slope}+R_d<R_{neg}$ which is equivalent to the intersection of the PWL AV characteristics of the resistor with the load line identical with horizontal axis $i\to0$. For the same impedance norm used above, we can observe a double-scroll attractor if

$$R_{neg}=10\text{ k}\Omega,\qquad R_{slope}=2\text{ k}\Omega. \quad (20)$$

Note that the voltage output of CFOA is buffered and directly represents the state variable $x(t)$.

We can approximate the PWL curve by a third-order polynomial function. For this purpose, two four-quadrant analog multipliers AD633 can be used, both with transfer function W=K(X1-X2)(Y1-Y2)+Z, where K=0.1. It is not hard to derive the analytic expression

$$i=f(u)=\frac{K^2}{R_a}u^3+\left(\frac{1}{R_a}-\frac{R_c}{R_dR_b}\right)u, \quad (21)$$

which generates a double-scroll attractor when

$$R_a=R_b=2.2\text{ k}\Omega,\quad R_c=12\text{ k}\Omega,\quad R_d=10\text{ k}\Omega. \quad (22)$$

Nonlinear oscillator works in hybrid voltage/current mode. Fig. 8 is an example of the time dependence of the chaotic waveform, namely $b(t)$ and $d(t)$. In the end, some oscilloscope HP54603B screenshots of selected chaotic attractors are presented in Fig. 9, making use of the XY view mode. Similarly, Fig. 10 shows a qualitatively equivalent chaotic structure for a polynomial nonlinearity. It is worth nothing that also Pspice circuit simulator gives us the same results for our oscillator with both types of the nonlinearity. Moreover, several other types of PWL AV characteristics can produce a chaotic waveform such as signum, sigmoid, goniometrical or exponential functions. For the first case, one can make use of a single comparator. The remaining functions are much more difficult to implement.

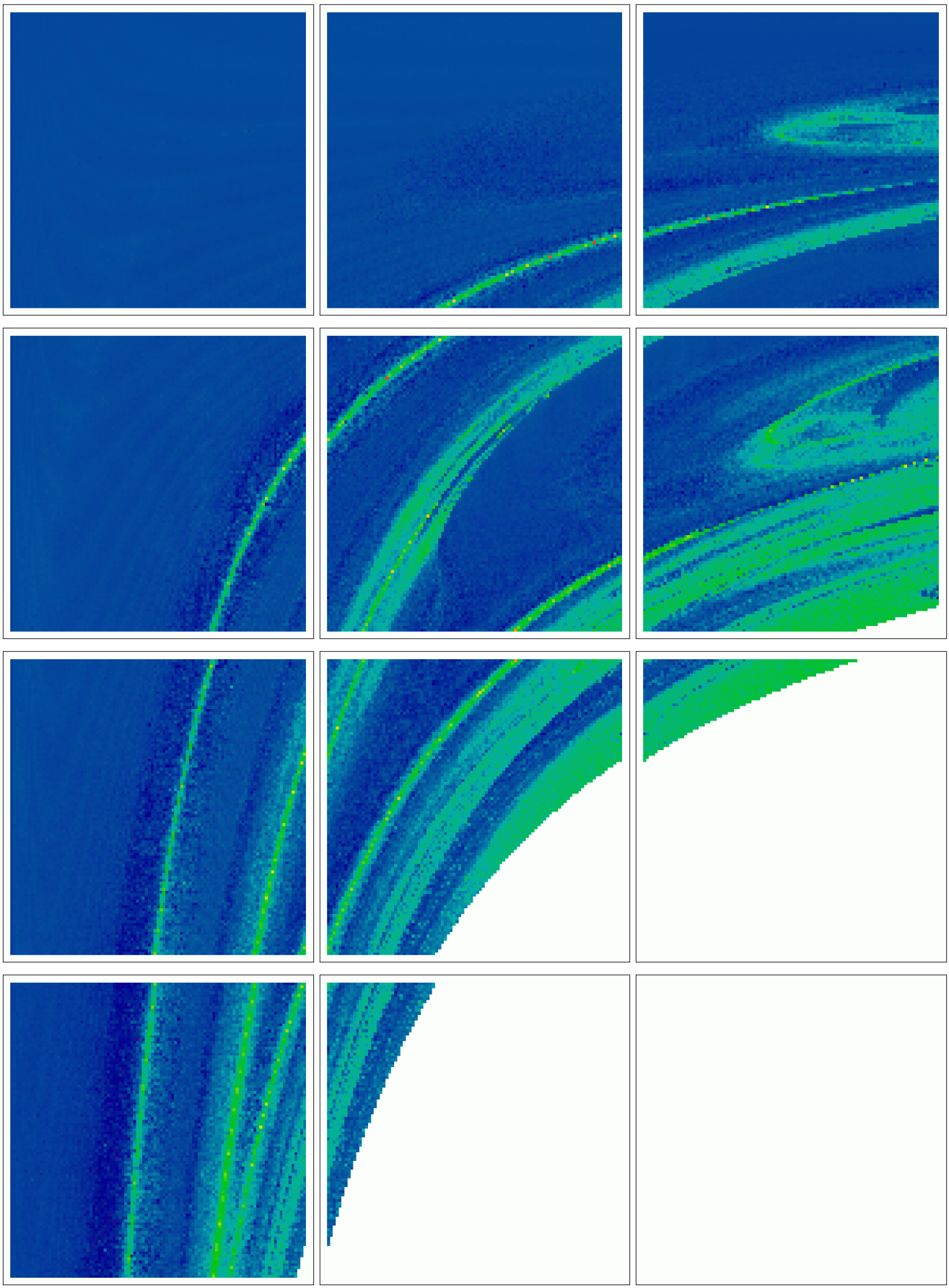

Fig. 1. Largest LE as a function of two internal system parameters: horizontal axis $p_3 \in (0, 3)$ and vertical axis $q_3 \in (-1, -5)$.

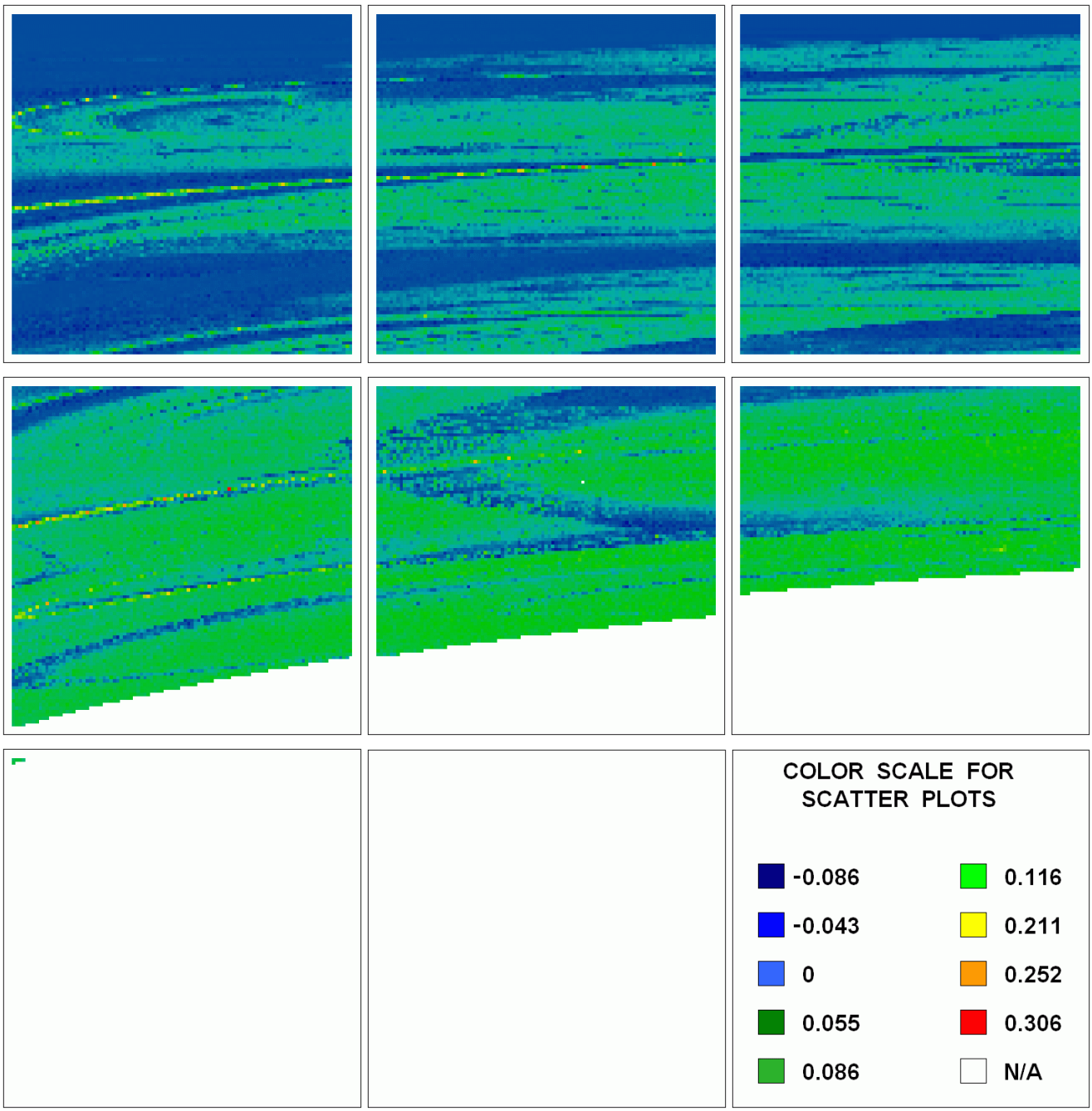

Fig. 2. Largest LE as a function of two internal system parameter: horizontal axis $p_3 \in (3, 6)$ and vertical axis $q_3 \in (-1, -3)$.

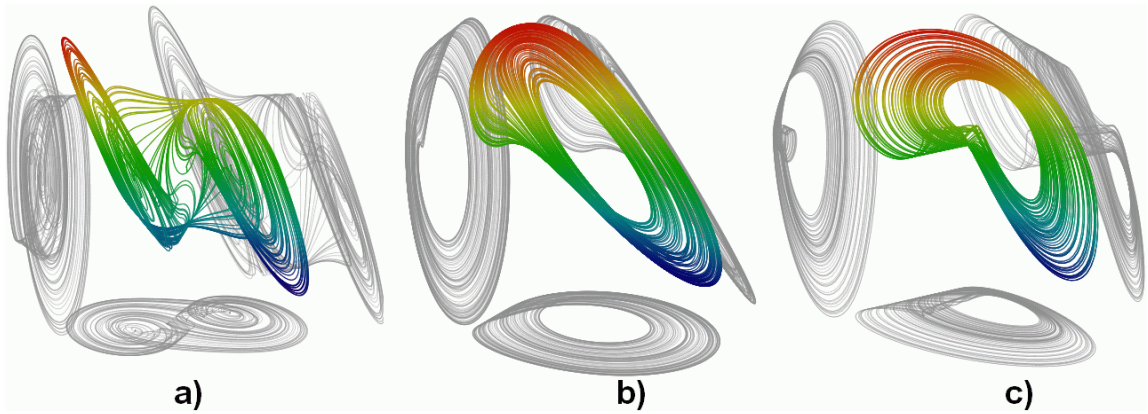

Fig. 3. Perspective views on different state space attractors: a) double-scroll b) funnel c) single-scroll.

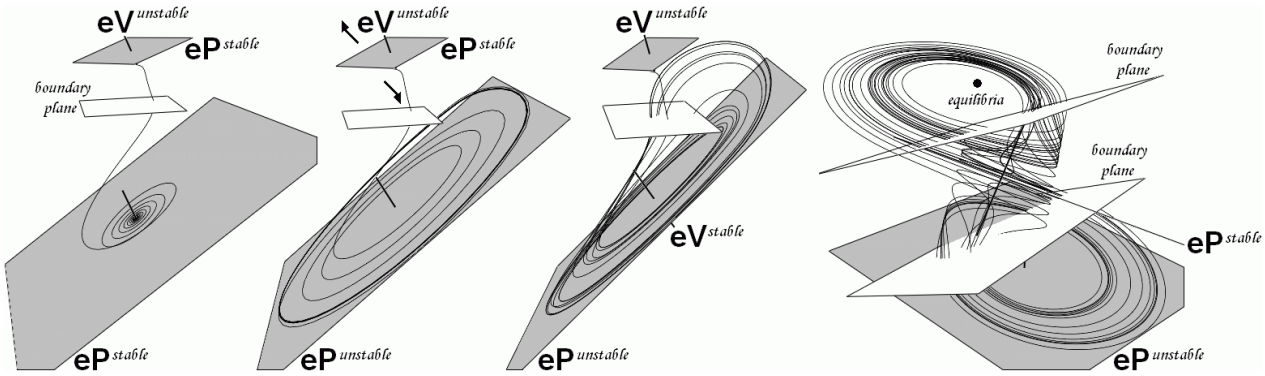

Fig. 4. Evolution of the double-scroll attractor with p_3=0.8 and: a) q_3=-0.4 b) q_3=-0.6 c) q_3=-0.8 d) q_3=-1.1.

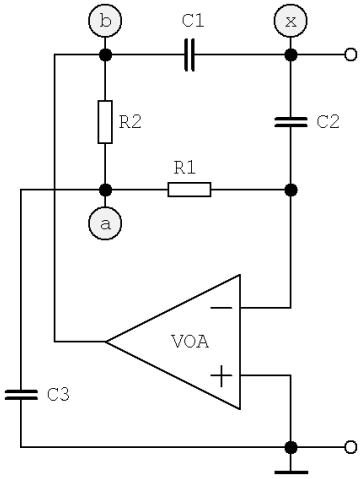

Fig. 5. Third-order admittance function Y(s).

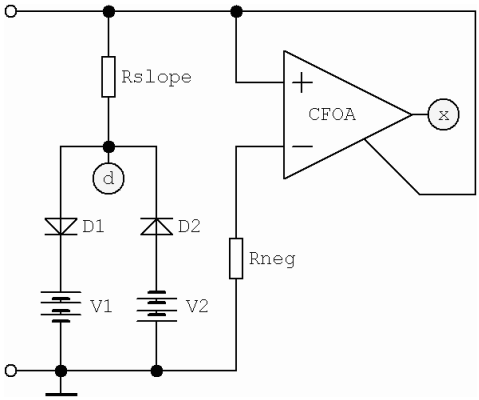

Fig. 6. Three-segment PWL resistor.

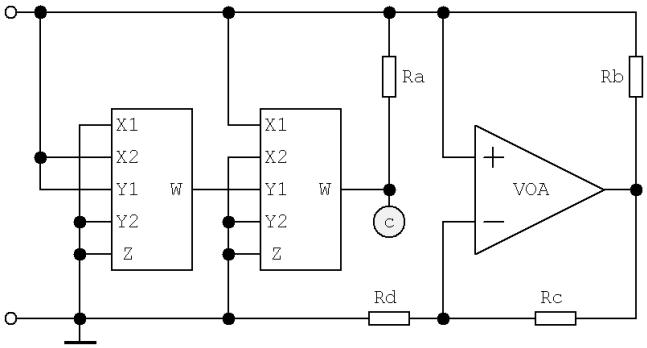

Fig. 7. Nonlinear resistor with polynomial AV characteristics.

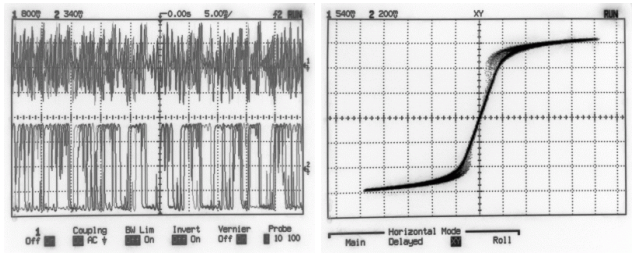

Fig. 8. Chaotic waveform in time domain, on-diode voltage.

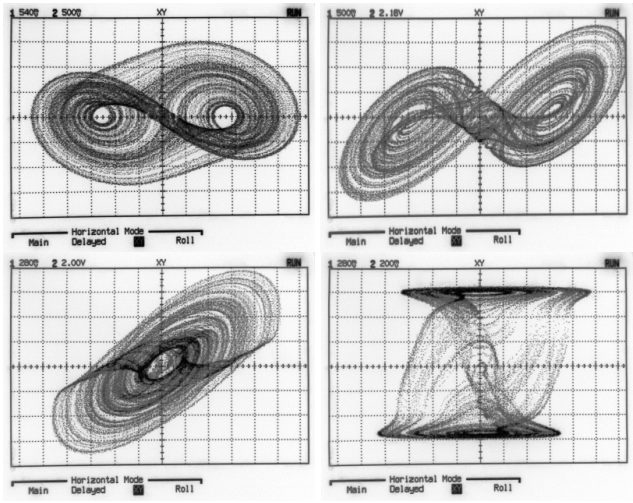

Fig. 9. Plane projections of selected chaotic steady states.

4. Conclusion

Although the nonlinear oscillator belongs to the dynamical systems of class C, it can not be realized by using a classical circuit synthesis, since it leads to the unrealistic values of circuit components [5]. The physical realization is very simple, removing the necessity of using cumbersome inductors with weakly defined inductance. Precise tuning of the circuit parameters allows us to observe different structures of chaotic attractors, corresponding transient events, periodical signals having a fundamental frequency as well as multiple-periodic harmonic waveforms. Practical measurements can prove a very good final agreement with theoretical expectations. Thus, this circuit is well suited for

laboratory experiments and educational purposed. During these measurements, we also verify that the chaotic signal has a continuous and broad-band frequency spectrum. This property can be used in many applications.

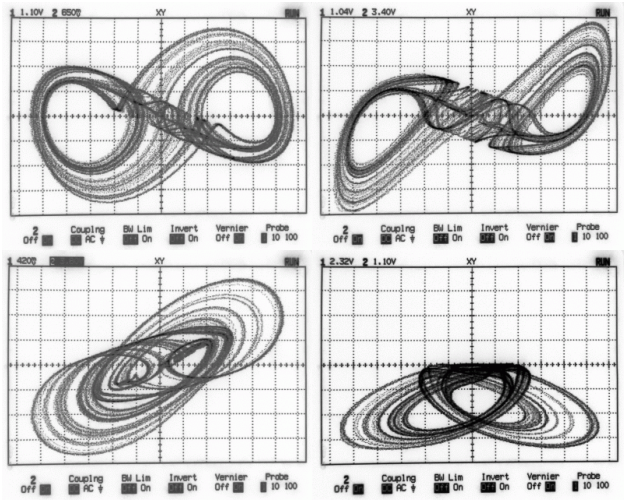

Fig. 10. Plane projections of selected chaotic steady states.

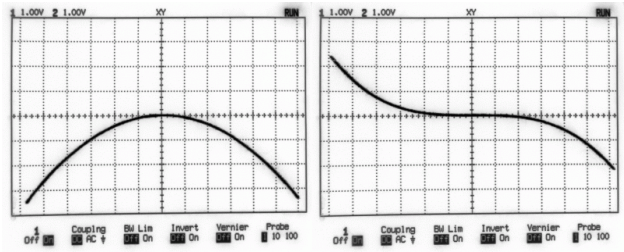

Fig. 11. Voltages at the output of both multipliers.

Acknowledgements

The research described in this paper was financially supported by the projects GAČR no. 102/03/H105, GAČR no. 102/04/0469 and MSM 021630513.

References

[1] CHUA, L. O., KOMURO, M., MATSUMOTO, T. The double scroll family. *IEEE Trans. on CAS I*, 1986, vol. 33, no. 11, p. 1073 – 1117.

[2] POSPÍŠIL, J., KOLKA, Z., HORSKÁ, J., BRZOBOHATÝ, J. New reference state model of the third-order piecewise-linear dynamical system. *Radioengineering*, 2000, vol. 9, no. 3, p. 1 – 4.

[3] SPROTT, J. C., LINZ, S. J. Algebraically simple chaotic flows. *International Journal of Chaos Theory and Applications*, 2000, vol. 5, no. 2, p. 1 – 20.

[4] POSPÍŠIL, J., KOLKA, Z., HORSKÁ, J., BRZOBOHATÝ, J. Simplest ODE equivalents of Chua's equations. *International Journal of Bifurcation and Chaos*, 2000, vol. 10, no. 1, p. 1 – 23.

[5] CHUA, L. O., LIN, G. N. Canonical realization of Chua's circuit family. *IEEE Trans. on CAS I,* 1990, vol. 37, no. 7, p. 885 – 902.

[6] SILVA, CH. P., CHUA, L. O. The overdamped double-scroll family. *International Journal of Circuit Theory and Applications*, 1988, vol. 16, p. 233 – 302.

[7] SILVA, CH. P. Shilnikov´s theorem – A tutorial. *IEEE Trans. on CAS I,* 1993, vol. 40, no. 10, p. 675 – 682.

About Authors…

Jiří PETRŽELA was born in Brno, Czech Republic, in 1978. Currently, he is a PhD. student at the Dept. of Radio Electronics with research interest focused on chaos and related topics.

Zdeněk KOLKA was born in Brno, Czech Republic, in 1969. At present, he is an Associate Professor at the Dept. of Radio Electronics. He is interested in PWL modeling, circuit simulation and nonlinear dynamical systems.

Stanislav HANUS was born in Brno, Czech Republic, in 1950. He is an Associate Professor at the Dept. of Radio Electronics with research interest concentrated on wireless and mobile communications.